CrossMark

The Open Cluster Chemical Abundances and Mapping Survey. VII. APOGEE DR17 [C/N]–Age Calibration

Taylor Spoo[1] , Jamie Tayar[2,3,15] , Peter M. Frinchaboy[1] , Katia Cunha[4,5], Natalie Myers[1] , John Donor[1],
Steven R. Majewski[6] , Dmitry Bizyaev[7,8] , D. A. García-Hernández[9,10] , Henrik Jönsson[11] , Richard R. Lane[12] ,
Kaike Pan[7] , Penélope Longa-Peña[13] , and A. Roman-Lopes[14]

[1] Department of Physics and Astronomy, Texas Christian University, TCU Box 298840, Fort Worth, TX 76129, USA; t.spoo@tcu.edu, p.frinchaboy@tcu.edu, n.myers@tcu.edu, j.donor@tcu.edu
[2] Institute for Astronomy, University of Hawai'i at Mānoa, 2680 Woodlawn Drive, Honolulu, HI 96822, USA
[3] Department of Astronomy, University of Florida, 211 Bryant Space Science Center, Gainesville, FL 32611, USA
[4] Observatório Nacional, Rua General José Cristino, 77, Rio de Janeiro, RJ 20921-400, Brazil
[5] Steward Observatory, University of Arizona, 933 North Cherry Avenue, Tucson, AZ 85721-0065, USA
[6] Department of Astronomy, University of Virginia, Charlottesville, VA 22904-4325, USA
[7] Apache Point Observatory and New Mexico State University, P.O. Box 59, Sunspot, NM 88349-0059, USA
[8] Sternberg Astronomical Institute, Moscow State University, Moscow, Russia
[9] Instituto de Astrofísica de Canarias, Vía Láctea S/N, E-38205 La Laguna, Tenerife, Spain
[10] Universidad de La Laguna, Departamento de Astrofísica, E-30206 La Laguna, Tenerife, Spain
[11] Materials Science and Applied Mathematics, Malmö University, SE-205 06 Malmö, Sweden
[12] Centro de Investigación en Astronomía, Universidad Bernardo O'Higgins, Avenida Viel 1497, Santiago, Chile
[13] Centro de Astronomía, Universidad de Antofagasta, Avenida Angamos 601, Antofagasta 1270300, Chile
[14] Department of Astronomy, Universidad La Serena, La Serena, Chile

Abstract

Large-scale surveys open the possibility to investigate Galactic evolution both chemically and kinematically; however, reliable stellar ages remain a major challenge. Detailed chemical information provided by high-resolution spectroscopic surveys of the stars in clusters can be used as a means to calibrate recently developed chemical tools for age-dating field stars. Using data from the Open Cluster Abundances and Mapping survey, based on the Sloan Digital Sky Survey/Apache Point Observatory Galactic Evolution Experiment 2 survey, we derive a new empirical relationship between open cluster stellar ages and the carbon-to-nitrogen ([C/N]) abundance ratios for evolved stars, primarily those on the red giant branch. With this calibration, [C/N] can be used as a chemical clock for evolved field stars to investigate the formation and evolution of different parts of our Galaxy. We explore how mixing effects at different stellar evolutionary phases, like the red clump, affect the derived calibration. We have established the [C/N]–age calibration for APOGEE Data Release 17 (DR17) giant star abundances to be $\log[\mathrm{Age(yr)}]_{\mathrm{DR17}} = 10.14\,(\pm0.08) + 2.23(\pm0.19)\,[\mathrm{C/N}]$, usable for $8.62 \leqslant \log(\mathrm{Age[yr]}) \leqslant 9.82$, derived from a uniform sample of 49 clusters observed as part of APOGEE DR17 applicable primarily to metal-rich, thin- and thick-disk giant stars. This measured [C/N]–age APOGEE DR17 calibration is also shown to be consistent with asteroseismic ages derived from Kepler photometry.

Unified Astronomy Thesaurus concepts: Open star clusters (1160); Galactic abundances (2002); Chemical abundances (224); Abundance ratios (11)

Supporting material: machine-readable table

1. Introduction

To understand our Galaxy's present-day structure, we need to learn how the Milky Way formed and evolved over time. To do this we need to be able to determine the ages of individual stars. However, ages are difficult to measure accurately for stars outside of star clusters. A common method to determine stellar ages is to compare key parameters, whether directly observed (e.g., colors and apparent magnitudes, the latter combined with parallaxes) or less directly inferred (e.g., $\log g$, T_{eff}), to those predicted from stellar evolution models, which allows accurate relative aging of stars, but this strategy is complicated due to

degeneracies in these parameters caused by chemical differences. Fortunately, several large-scale spectroscopic surveys systematically collecting high-resolution data, such as the Apache Point Observatory Galactic Evolution Experiment survey (APOGEE; Abdurro'uf et al. 2022), the Gaia-ESO public spectroscopic survey (Gilmore et al. 2012), and the Galactic Archaeology with HERMES survey (GALAH; Martell et al. 2017), are providing detailed and precise chemical abundances for multiple chemical elements spanning millions of stars across various Galactic stellar populations, including star clusters. Apart from providing essential information to break the age-dating degeneracies, these spectroscopic surveys provide additional key parameters, such as Li depletion (e.g., Gao et al. 2018; Magrini et al. 2021, and references therein) or carbon-to-nitrogen ([C/N]) abundance ratios (e.g., Bertelli Motta et al. 2017; Casali et al. 2019; Hasselquist et al. 2019) that are alternative, chemistry-based diagnostics of stellar age.

---

[15] NASA Hubble Fellow.

A natural ally in calibrating [C/N] ages is asteroseismology, now being generated for large numbers of stars through space missions like CoRoT (Auvergne et al. 2009), Kepler (Borucki et al. 2010), and TESS (Ricker et al. 2015). Asteroseismology uses high-precision photometry to measure frequency modes in stars that are dependent on the structure, and therefore mass, of the star. Ages for red giant branch (RGB) stars can be derived using asteroseismic photometric measurements from Kepler and TESS because the mass of RGB stars correlates with age. For example, utilizing combined data from Kepler and the APOGEE survey, the APOKASC catalog (Pinsonneault et al. 2018) has measured masses, and thereby ages, for ∼7000 evolved stars.

Such masses and ages have been shown previously to correlate with [C/N] (Martig et al. 2016; Ness et al. 2016). However, to obtain their exact absolute calibration is challenging (Gaulme et al. 2016; Huber et al. 2017; Zinn et al. 2019), as is controlling for physical (e.g., mass loss) and systematic differences. Thus, it is worthwhile searching for independent strategies for [C/N]–age calibration.

Star clusters have long been one of the key test beds of our understanding of stellar evolution and stellar physics, empirically demonstrating what properties stars of the same chemistry and age should have. In particular, open clusters are useful objects for calibrating the relationship between age and [C/N], because star clusters are the most reliable age-datable tracers, and open clusters also have ages that span the history of the Galactic disk, from currently forming stars up to systems 9–10 Gyr old. Cluster ages can be accurately determined, using the best-measured and best-understood stars in the cluster, by the location of the main-sequence turnoff (MSTO) on a H-R diagram.

Carbon and nitrogen abundances in evolved stars on the RGB will change due to the first dredge-up, where material from regions that have previously undergone nuclear burning are brought to the surface. The changes in the balance of carbon and nitrogen in the surface are dependent on stellar mass (Masseron & Gilmore 2015; Martig et al. 2016; Ness et al. 2016). With open cluster studies, we can therefore empirically calibrate a relationship between stellar ages, exploiting the precise ages determined by cluster MSTO isochrone fitting, and precise [C/N] abundances measured for the RGB stars in these systems.

Casali et al. (2019) have investigated this relationship using a compilation of nearly 40 open clusters using a combined data set from the Gaia-ESO survey and the APOGEE Data Release 14 (DR14) survey. However, these results relied on a smaller number of clusters studied heterogeneously, which opens the possibility of systematics that could bias the results.

With the availability of much more APOGEE data via the Sloan Digital Sky Survey (SDSS) DR17—including the addition of southern hemisphere stars and clusters—we are in a position to improve upon the Casali et al. (2019) effort to calibrate empirically a relationship between [C/N] abundances of RGB stars and their ages using a homogeneous data set of chemical abundance measurements for open cluster RGB stars deriving entirely from APOGEE spectroscopy. Using the ages determined by Cantat-Gaudin et al. (2020) for clusters that are in SDSS/APOGEE DR17 as defined by the Open Cluster Chemical Abundances and Mapping (OCCAM) Survey (Myers et al. 2022, submitted), we calibrate a relationship between [C/N] and stellar age for stars that have experienced the first

dredge-up. We separate the RGB and red clump (RC) stars to investigate the effects that stellar evolution may have on the calibration for stellar age. We also compare our results to those from previous work, in particular from the APOKASC asteroseismology method for determining stellar ages. These improvements in the [C/N]–age calibration will help increase the power of large-scale, high-resolution stellar spectroscopic surveys like APOGEE to explore Galactic chemodynamical evolution using a reliable means to benchmark ages for vast numbers of stars.

2. Data and Analysis

2.1. SDSS/APOGEE Survey

This study makes use of the APOGEE surveys (APOGEE-1 and -2; Majewski et al. 2017; S. R. Majewski et al. 2022, in preparation) that are part of the SDSS III and IV (Eisenstein et al. 2011; Blanton et al. 2017), respectively. Data were taken with the 2.5 m Sloan Foundation Telescope (Gunn et al. 2006) at the Apache Point Observatory and the 2.5 m du Pont telescope (Bowen & Vaughan 1973) at the Las Campanas Observatory, using the APOGEE-North and APOGEE-South spectrographs (Wilson et al. 2019), respectively. APOGEE Target selection is described in Zasowski et al. (2013, 2017), Beaton et al. (2021), and Santana et al. (2021), with open cluster targeting further detailed in Frinchaboy et al. (2013) and Donor et al. (2018).

The APOGEE spectra were reduced using the APOGEE reduction pipeline (Nidever et al. 2015), and key parameters were derived automatically via the APOGEE Stellar Parameters and Chemical Abundances Pipeline (ASPCAP; García Pérez et al. 2016). As the basis of the spectral analysis large grids of synthetic spectra are calculated (Zamora et al. 2015) using stellar atmospheric models (Mészáros et al. 2012) and an updated line list with astrophysically tuned and vetted atomic and molecular data (Smith et al. 2021; see also Shetrone et al. 2015). Many aspects of these parts of the data analysis have been updated during the years of the survey and are described in Holtzman et al. (2015, 2018), Jönsson et al. (2018, 2020), Smith et al. (2021), and J. Holtzman et al. (2022, in preparation). These continuing analysis updates result in the possibility that the determined stellar parameters and abundances may change for a particular star from one data release to another. In DR17, ASPCAP reports stellar parameters and chemical abundances for more than 20 elements. This includes the abundances of carbon and nitrogen, which can be more challenging to measure from optical spectra. However, APOGEE is uniquely suited to reliably measuring the C, N, and O abundances, derived through the combined analysis of their contributions to numerous molecular bands of CN, CO, and OH. These particular molecular lines are fully described in Smith et al. (2021).

2.1.1. SDSS/APOGEE Survey DR17

In this work, we use data from the latest, and final, data release of the Apache Point Observatory Galactic Evolution Experiment 2 (APOGEE-2) survey. The APOGEE-2 DR17 (Abdurro'uf et al. 2022) includes all observations from both APOGEE spectrographs taken from 2011 August to 2021 January and has ∼734,000 stars. A full description of the APOGEE DR17 data quality and parameter limitations will be presented in Abdurro'uf et al. (2022) and J. Holtzman et al.

(2022, in preparation). The most significant update in the ASPCAP analysis code for DR17 compared to that used in previous data releases is that the library of synthetic spectra was calculated using the Synspec code (e.g., Hubeny et al. 2021). Synspec allows for the non-local thermodynamic equilibrium (non-LTE) line formation in a plane parallel geometry. However, in DR17 only the elements Na, Mg, K, and Ca were computed in non-LTE (Osorio et al. 2020), while the remaining elements studied by APOGEE, including C and N, were still computed in LTE. That said, the determined C and N abundances—and hence [C/N]—can be different in DR17 from prior data releases, even in cases where the same spectra are analyzed, because the DR14 and DR16 APOGEE data releases relied on the Turbospectrum code (Plez 2012), which, while not accommodating non-LTE populations to be specified, does compute atmospheres within a spherical geometry (Gustafsson et al. 2008). For the interested reader, the choice of the model atmospheres and compositions between the various options is described more fully in Abdurro'uf et al. (2022) and J. Holtzman et al. (2022, in preparation).

2.1.2. OCCAM Survey Catalog

This work uses data from the OCCAM survey (Frinchaboy et al. 2013; Cunha et al. 2015; Donor et al. 2018, 2020). The DR17 OCCAM data set (Myers et al. 2022, submitted) includes APOGEE data from 153 open clusters with a total number of 2061 stars determined to be likely members. From this parent catalog, Myers et al. select only 94 clusters determined to be "highly reliable" for use in studying Galactic chemical trends, and we refer the reader to Donor et al. (2018, 2020) for a full description of member selection and explanation of how the "highly reliable" sample was selected. We utilize only data from the "highly reliable" OCCAM DR17 value-added catalog (VAC[16]).

2.2. Cluster Member Sample Selection

To select stars having reliable C and N measurements for our analysis, we used ASPCAP bit-wise flags for removing unreliable C and N abundances, along with a requirement that the spectra from which they were derived have a signal-to-noise ratio greater than 70. The bit-wise flags are fully described in Jönsson et al. (2020) and J. Holtzman et al. (2022, in preparation). In addition, we crossmatched our sample with the double-lined spectroscopic binary (SB2) catalog (Kounkel et al. 2021) to check whether any stars in our sample were SB2s, and found none to be SB2s.

We also made a cut to our sample based on OCCAM membership probabilities in radial velocity, proper motion, and metallicity. To provide a more reliable sample, we selected with a tighter requirement of >30% membership probability in radial velocity, proper motion, and metallicity.

In addition, we selected stars that lie within a radius 2 times larger than the radius containing half the members (r_{50}) as determined by Cantat-Gaudin et al. (2020). These combined criteria provide a well-vetted and pure sample that compares well to other cluster membership catalogs (e.g., Cantat-Gaudin et al. 2020). Because [C/N] abundances only correlate with age for evolved stars, we applied a surface gravity cut to ensure we were obtaining evolved stars that have experienced the first

---

[16] https://www.sdss.org/dr17/data_access/value-added-catalogs/?vac_id=open-cluster-chemical-abundances-and-mapping-catalog

Table 1
Stellar Data Quality Selection Criteria

Source	Parameter	Selection
APOGEE Data Quality Cuts		
APOGEE/DR17	STARFLAG—Stellar Parameters	$!=16$
APOGEE/DR17	ASPCAP C Flag	$!=21$
APOGEE/DR17	ASPCAP N Flag	$!=22$
APOGEE/DR17	ASPCAP Flag—Chemistry	$!=23$
APOGEE/DR17	VSCATTER (km s^{-1})	<1
APOGEE/DR17	SNREV	>70
Cluster Membership Cuts		
Myers et al. (2022, submitted)	RV_PROB	>0.3
Myers et al. (2022, submitted)	FEH_PROB	>0.3
Myers et al. (2022, submitted)	PM_PROB	>0.3
Cantat-Gaudin et al. (2020)	$\sqrt{((l_* - l_{CG})\cos(b_{CG}))^2 + (b_* - b_{CG})^2}$	$<2 \times$ r50
Stellar Evolutionary Cuts		
APOGEE/DR17	LOGG	<3.3

Note. The table summarizes the various selection criteria applied to the stars within clusters common between Cantat-Gaudin et al. (2020) and the OCCAM survey VAC (Myers et al. 2022, submitted) to ensure that only cluster stars whose properties are well measured and for which the [C/N] ratios should be correlated with age. STARFLAG and ASPCAP bit-wise flags are described in https://www.sdss.org/dr17/irspec/apogee-bitmasks/.

---

dredge-up. Based on a combination of stellar models and the APOKASC data, we included only stars with $\log g < 3.3$, which should represent the post-dredge-up stars and the age studies here. Next, from our uniform sample, we used the APOGEE DR17 RC catalog (Bovy et al. 2014; J. Bovy et al. 2022, in preparation) to flag likely RC stars within our sample; this will allow us to investigate RC mixing effects that could skew the age calibration. Likely RC stars included in the APOGEE DR17 RC catalog were selected based on their location within color, metallicity, surface gravity, and effective temperature space, with details fully described in Bovy et al. (2014).

The sample selection criteria adopted are listed in Table 1. After applying this criteria, our sample comprises 75 clusters given in Table 2, which includes cluster names, cluster ages as reported by Cantat-Gaudin et al. (2020), DR17 median [Fe/H] abundances, and median [C/N] abundances for the member stars with good measurements. Median elemental abundance uncertainties were calculated using the standard error of the mean.

2.3. Systematics between DR14, DR16, and DR17

During the course of the APOGEE survey, the APOGEE team has made improvements to the automated analysis pipeline. For each APOGEE data release there have been changes and improvements to, for example, the atomic and molecular line lists, stellar atmosphere models, implementation of the code, etc, as discussed in Section 2.1. In order to compare our work with results from other studies that used previous APOGEE data releases (e.g., Casali et al. 2019, which partially used DR14 data), we briefly investigate systematic

Table 2
Mean [C/N] DR17 Abundance—Full Sample

Cluster[a] Name	log(Age)[b] (yr)	[Fe/H] (dex)	[C/N] (dex)	DR17 Memb.
Berkeley 17	**9.86**	**−0.183**	**−0.164 ± 0.010**	**8**
Berkeley 18	**9.64**	**−0.385**	**−0.332 ± 0.015**	**18**
Berkeley 19	9.34	−0.361	−0.517 ± 0.000	1
Berkeley 2	**8.77**	**−0.208**	**−0.366 ± 0.048**	**6**
Berkeley 20	9.68	−0.432	−0.372 ± 0.000	1
Berkeley 21	**9.33**	**−0.269**	**−0.355 ± 0.006**	**3**
Berkeley 29	**9.49**	**−0.527**	**−0.280 ± 0.009**	**2**
Berkeley 31	**9.45**	**−0.426**	**−0.278 ± 0.001**	**2**
Berkeley 33	8.37	−0.243	−0.560 ± 0.000	1
Berkeley 53	**8.99**	**−0.121**	**−0.517 ± 0.025**	**6**
Berkeley 53	**8.99**	**−0.121**	**−0.517 ± 0.025**	**6**
Berkeley 66	**9.49**	**−0.215**	**−0.302 ± 0.008**	**5**
Berkeley 71	**8.94**	**−0.232**	**−0.519 ± 0.029**	**5**
Berkeley 75	**9.23**	**−0.412**	**−0.504 ± 0.039**	**3**
Berkeley 85	**8.62**	**+0.064**	**−0.420 ± 0.009**	**10**
Berkeley 9	9.14	−0.180	−0.624 ± 0.000	1
Berkeley 91	8.80	+0.070	−0.327 ± 0.000	1
Berkeley 98	**9.39**	**−0.044**	**−0.376 ± 0.043**	**5**
Czernik 20	**9.22**	**−0.177**	**−0.400 ± 0.049**	**4**
Czernik 21	**9.41**	**−0.326**	**−0.280 ± 0.008**	**2**
Czernik 23	8.43	−0.329	−0.571 ± 0.000	1
Czernik 30	**9.46**	**−0.387**	**−0.348 ± 0.017**	**2**
ESO 211 03	**9.11**	**+0.107**	**−0.447 ± 0.031**	**4**
FSR 0494	**8.95**	**−0.021**	**−0.515 ± 0.015**	**5**
FSR 0496	9.31	−0.137	−0.429 ± 0.000	1
FSR 0667	8.85	−0.034	−0.544 ± 0.000	1
FSR 0716	8.94	−0.385	−0.398 ± 0.000	1
FSR 0937	**9.08**	**−0.371**	**−0.439 ± 0.032**	**2**
FSR 1113	9.44	−0.347	−0.237 ± 0.000	1
Haffner 4	8.66	−0.182	−0.482 ± 0.000	1
IC 1369	8.46	−0.112	−0.560 ± 0.024	3
IC 166	**9.12**	**−0.095**	**−0.488 ± 0.037**	**13**
King 15	8.47	−0.128	−0.457 ± 0.000	1
King 2	9.61	−0.184	−0.292 ± 0.000	1
King 5	**9.01**	**−0.159**	**−0.464 ± 0.013**	**4**
King 7	8.35	−0.162	−0.366 ± 0.073	7
King 8	8.92	−0.239	−0.469 ± 0.000	1
Melotte 71	**8.99**	**−0.151**	**−0.478 ± 0.020**	**3**
NGC 1193	**9.71**	**−0.345**	**−0.255 ± 0.026**	**3**
NGC 1245	**9.08**	**−0.089**	**−0.480 ± 0.017**	**25**
NGC 136	8.41	−0.266	−0.457 ± 0.000	1
NGC 1664	8.71	−0.060	−0.564 ± 0.000	1
NGC 1798	**9.22**	**−0.279**	**−0.429 ± 0.017**	**10**
NGC 1817	**9.05**	**−0.157**	**−0.402 ± 0.045**	**5**
NGC 1857	8.40	−0.176	−0.414 ± 0.013	2
NGC 188	**9.85**	**+0.064**	**−0.244 ± 0.010**	**32**
NGC 1907	**8.77**	**−0.126**	**−0.506 ± 0.046**	**3**
NGC 1912	**8.47**	**−0.169**	**−0.435 ± 0.016**	**2**
NGC 2158	**9.19**	**−0.246**	**−0.342 ± 0.013**	**41**
NGC 2204	**9.32**	**−0.280**	**−0.423 ± 0.021**	**20**
NGC 2243	**9.64**	**−0.458**	**−0.338 ± 0.037**	**6**
NGC 2304	**8.96**	**−0.141**	**−0.400 ± 0.009**	**2**
NGC 2324	**8.73**	**−0.221**	**−0.517 ± 0.037**	**4**
NGC 2420	**9.24**	**−0.205**	**−0.337 ± 0.012**	**16**
NGC 2447	**8.76**	**−0.114**	**−0.548 ± 0.016**	**3**
NGC 2479	8.99	−0.049	−0.436 ± 0.000	1
NGC 2682	**9.63**	**+0.000**	**−0.368 ± 0.011**	**19**
NGC 4337	**9.16**	**+0.222**	**−0.491 ± 0.012**	**6**
NGC 6705	8.49	+0.096	−0.440 ± 0.016	12
NGC 6791	**9.80**	**+0.313**	**−0.165 ± 0.010**	**41**
NGC 6811	**9.03**	**−0.051**	**−0.521 ± 0.012**	**6**
NGC 6819	**9.35**	**+0.040**	**−0.352 ± 0.019**	**42**
NGC 6866	**8.81**	**+0.010**	**−0.565 ± 0.030**	**2**

Table 2
(Continued)

Cluster[a] Name	log(Age)[b] (yr)	[Fe/H] (dex)	[C/N] (dex)	DR17 Memb.
NGC 7062	8.63	−0.023	−0.569 ± 0.000	1
NGC 752	**9.07**	**−0.064**	**−0.442 ± 0.010**	**5**
NGC 7789	**9.19**	**−0.032**	**−0.421 ± 0.011**	**65**
Ruprecht 147	**9.48**	**+0.116**	**−0.395 ± 0.030**	**3**
Ruprecht 82	8.66	−0.037	−0.702 ± 0.000	1
Teutsch 10	8.79	−0.350	−0.638 ± 0.000	1
Teutsch 12	**8.92**	**−0.200**	**−0.569 ± 0.031**	**4**
Teutsch 51	**8.83**	**−0.332**	**−0.524 ± 0.011**	**3**
Teutsch 84	9.02	+0.200	−0.506 ± 0.000	1
Tombaugh 2	**9.21**	**−0.371**	**−0.605 ± 0.070**	**4**
Trumpler 20	**9.27**	**+0.105**	**−0.509 ± 0.017**	**25**
Trumpler 5	**9.63**	**−0.449**	**−0.274 ± 0.018**	**8**

Notes.
[a] Bold denotes clusters in the final calibration sample.
[b] All ages come from Cantat-Gaudin et al. (2020) and the log(Age) errors are equal to 0.1.

differences between the carbon and nitrogen abundance results derived from the different APOGEE data releases.

The APOGEE-2 DR14 (Abolfathi et al. 2018) included observations from 2011 August to 2016 July and has ∼263,000 stars. DR14 APOGEE data includes data from the APOGEE-1 and first two years of the APOGEE-2 North survey, all taken from the Apache Point Observatory. A full description of the APOGEE DR14 data quality and parameter limitations is presented in Holtzman et al. (2018) and Jönsson et al. (2018). The APOGEE-2 DR16 (Ahumada et al. 2020) included observations from 2011 August to 2018 August and has ∼473,000 stars. DR16 APOGEE data included data from the APOGEE-1 and first four years of the APOGEE-2 North survey taken from the Apache Point Observatory, plus the first year of APOGEE-2 South data taken from the Las Campanas Observatory. A full description of the APOGEE DR16 data quality and parameter limitations is presented in Jönsson et al. (2020).

We find a global offset of [Fe/H] between DR14 and DR17 as well as for DR16 and DR17 to be 0.07 and 0.02 dex, respectively. This investigation for differences between previous releases for metallicity ([Fe/H]), α elements (O, Mg, Si, S, Ca, Ti), iron-peak elements (V, Cr, Mn, Co, Ni), and other elements (Na, Al, K) is discussed in detail in Donor et al. (2020) and Myers et al. (2022, submitted).

The top panels of Figure 1 compare the C and N abundances for stars in the 75 cluster sample that have abundances in both DR14 and DR17. The median change for C is measured to be −0.029 dex with a scatter of 0.047 dex and the median change for N is measured to be +0.081 dex with a scatter of 0.052 dex. Similarly, the bottom panels of Figure 1 compare the C and N abundances for stars in the 75 cluster sample that have abundances in both DR16 and DR17. The median change for C is measured to be +0.065 dex with a scatter of 0.039 dex and the median change for N is measured to be −0.013 dex with a scatter of 0.051 dex. These systematic offsets between the compared data releases are due to changes within the SDSS data reduction pipeline, as discussed in Section 2.1.1. This simple analysis demonstrates that it is not appropriate or straightforward to intercompare [C/N]–age relations derived
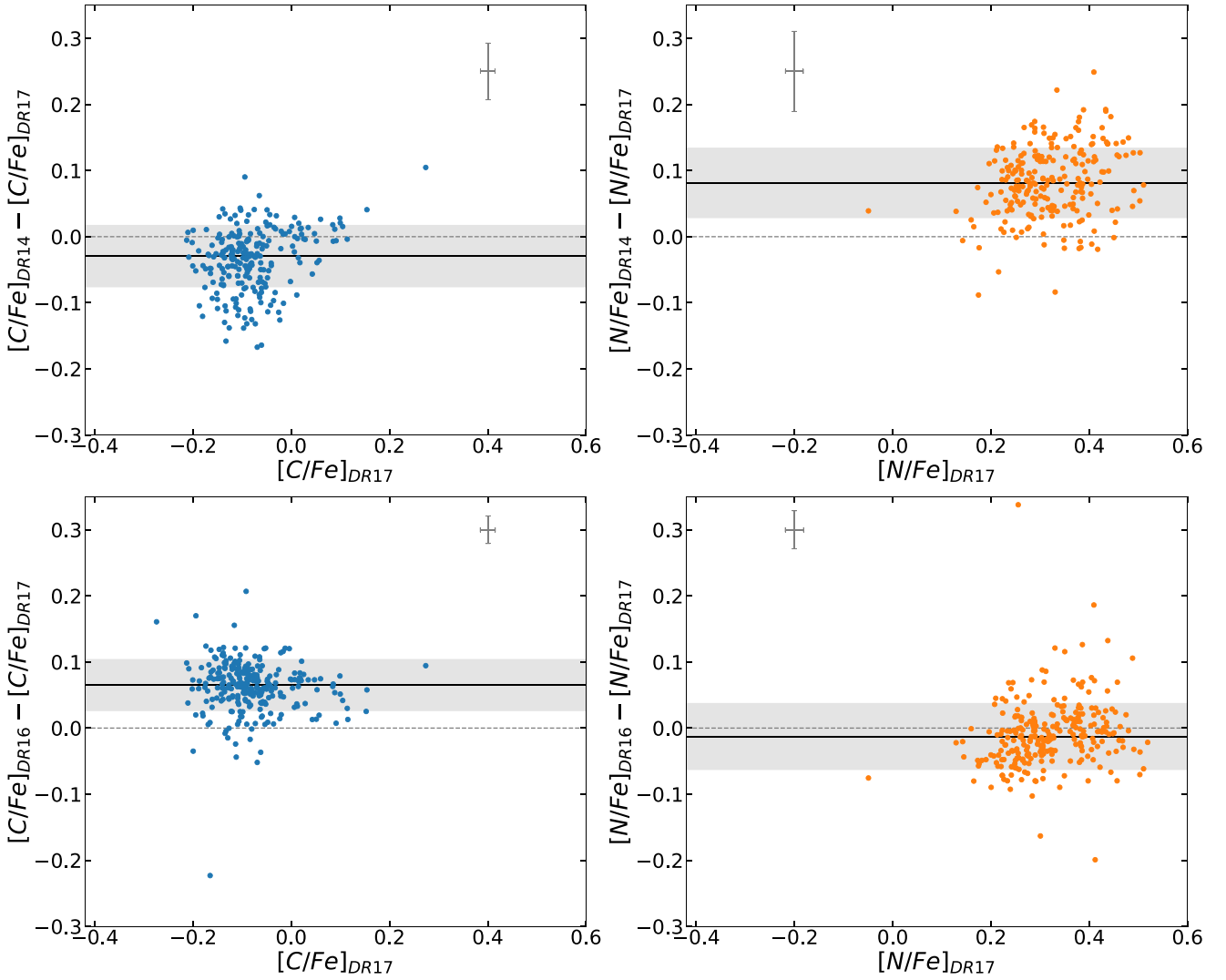
Figure 1. C and N abundance comparisons between different APOGEE data releases: DR14 to DR17 (top panels), and DR16 to DR17 (bottom labels). A representative error bar is shown in each panel. The horizontal black line represents the median change. A gray shaded region is shown in each plot to represent the scatter on the median.

from different APOGEE data releases, unless one accounts for these simple, though systematic, variations in APOGEE carbon and nitrogen abundances over time.

3. Results and Discussion

3.1. Final Cluster Sample

After application of the various selection criteria summarized in Table 1, our sample comprises 75 clusters with 577 member stars. Figure 2 shows the [C/N] abundance ratios versus cluster age for that sample. To ensure our calibration is reliable, we excluded clusters that contained only one member (those shown with a red diamond), as well as those having $\log(Age[yr]) < 8.5$ (dark blue squares). As apparent in Figure 2, clusters younger than $\log(Age[yr]) = 8.5$ do not seem to follow the same trend in [C/N] and $\log(Age[yr])$.

Other than possible observational issues related to the analysis of young stars (Baratella et al. 2020; Spina et al. 2020), there are likely two effects at play that affect the more massive
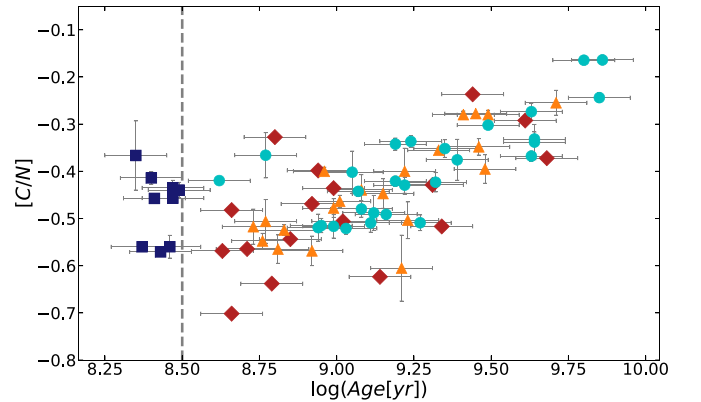
Figure 2. The [C/N] vs. log(Age[yr]) distribution for clusters common to the OCCAM Survey and Cantat-Gaudin sample, which includes 75 clusters. Young clusters, log(Age) ⩽ 8.5, are represented with navy squares. Clusters marked with a red diamond are those with only one stellar member after cuts are applied. Clusters with two to four stellar members are represented by orange triangles, and those with five or more stellar members are represented by cyan circles.
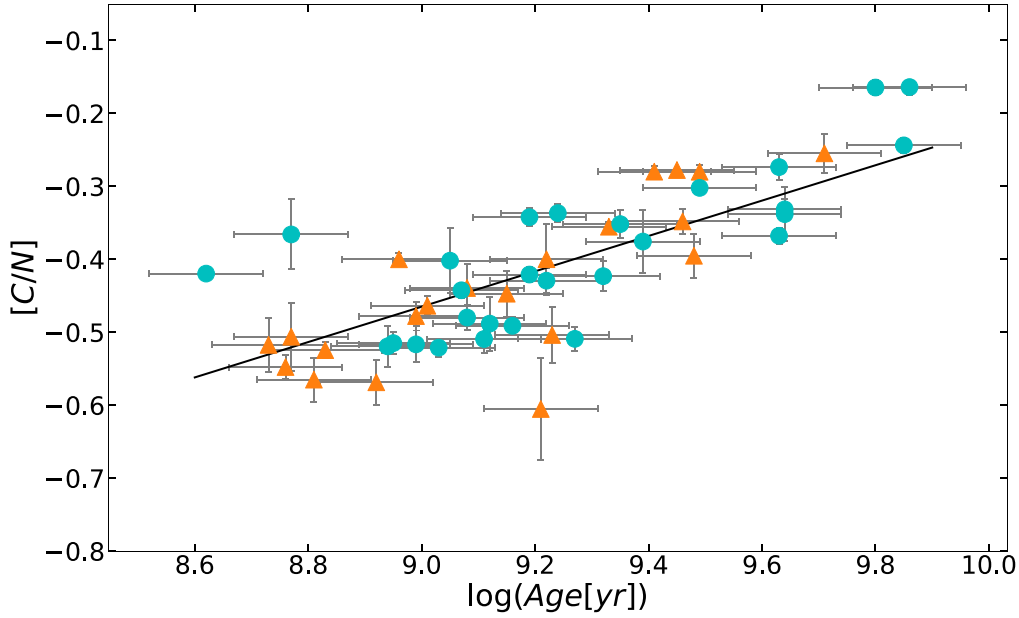
Figure 3. The [C/N] vs. log(Age[yr]) distribution for the final sample, composed of clusters common to the OCCAM Survey and Cantat-Gaudin sample, totaling 49 clusters. Clusters with two to four stellar members are represented by orange triangles, and those with five or more stellar members are by cyan circles.

Table 3
Full Calibration Cluster Sample Stellar Data from APOGEE DR17

Cluster Name	2MASS ID	T_{eff} (K)	$\log(g)$ (dex)	[Fe/H] (dex)	[C/N] (dex)	RC?[a] Label
Berkeley 17	2M05195385+3035095	4665 ± 9	2.60 ± 0.03	-0.12 ± 0.01	-0.23 ± 0.02	N
Berkeley 17	2M05202118+3035544	4799 ± 9	2.47 ± 0.02	-0.15 ± 0.01	-0.16 ± 0.02	N
Berkeley 17	2M05202905+3032414	4783 ± 13	2.84 ± 0.03	-0.20 ± 0.01	-0.18 ± 0.03	N
Berkeley 17	2M05203121+3035067	4820 ± 9	2.49 ± 0.02	-0.19 ± 0.01	-0.14 ± 0.02	N
Berkeley 17	2M05203650+3030351	4444 ± 6	1.98 ± 0.02	-0.17 ± 0.01	-0.15 ± 0.02	N
Berkeley 17	2M05203799+3034414	4307 ± 6	1.93 ± 0.02	-0.18 ± 0.01	-0.16 ± 0.02	N
Berkeley 17	2M05204143+3036042	4824 ± 9	2.49 ± 0.03	-0.22 ± 0.01	-0.14 ± 0.02	Y
Berkeley 17	2M05204488+3038020	4807 ± 8	2.43 ± 0.02	-0.21 ± 0.01	-0.21 ± 0.02	Y
Berkeley 18	2M05211671+4533170	4220 ± 6	1.43 ± 0.02	-0.40 ± 0.01	-0.32 ± 0.02	N
Berkeley 18	2M05214927+4525225	5126 ± 19	2.65 ± 0.04	-0.33 ± 0.01	-0.26 ± 0.05	Y
Berkeley 18	2M05215476+4526226	4309 ± 6	1.56 ± 0.03	-0.40 ± 0.01	-0.35 ± 0.02	N

...

Note.
[a] "Y" is an identified red clump star using the APOGEE DR17 red clump value-added catalog (Bovy et al. 2014). "N" denotes stars not identified as part of the catalog and considered red giant branch stars.

(This table is available in its entirety in machine-readable form.)

evolved stars ($M \geqslant 2.5\,M_\odot$) in these young clusters that are not present in the lower-mass evolved stars of older clusters. The first is that massive stars spend less time on the first ascent RGB and proportionally more time in the core He-burning phase (Iben 1967a; Danchi et al. 2006). These young clusters therefore are likely dominated by stars that have already undergone a weakly degenerate or nondengeneate helium ignition and it is not yet clear whether such an event could drive additional mixing that would alter their surface abundances. Second, in more massive stars the first dredge-up reaches deeper (e.g., Iben 1964, 1965, 1967a, 1967b) into regions where the carbon–nitrogen–oxygen (CNO) cycle was significant in prior evolutionary phases. This means that the material being dredged up has a fixed ratio of carbon and nitrogen, which is at an equilibrium set by the nuclear reaction

times of the CNO cycle (Dearborn & Eggleton 1976; Dearborn et al. 1976). Since this ratio is not changing with mass, the relationship between the [C/N] ratio after the dredge-up and the stellar mass becomes much weaker, making it less sensitive as an age diagnostic. Given these two caveats, we have excluded these stars from fits in this paper, but encourage more careful studies of stars in this regime in the future.

After the application of these additional membership and cluster age cuts the sample used for our [C/N]–age calibration (Figure 3) comprises 49 clusters (530 stars), covering an age range of $8.62 \leqslant \log(\mathrm{Age[yr]}) \leqslant 9.82$ and a metallicity range of $-0.53 \leqslant [\mathrm{Fe/H}] \leqslant 0.31$. The individual stars from the calibration sample are listed in Table 3. Table 2 shows these calibration clusters in bold.
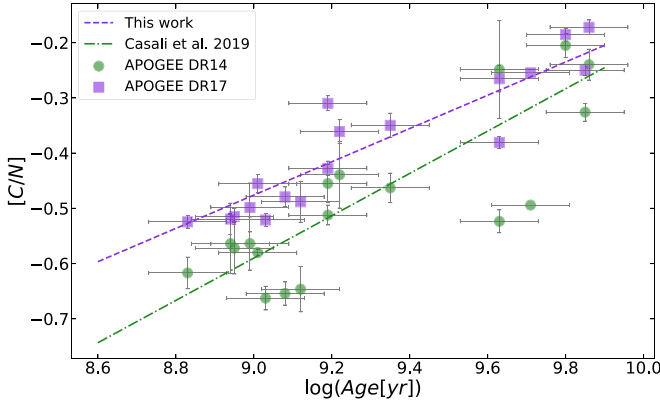
Figure 4. Median [C/N] ratio of open cluster star members, as derived in DR14 (green circles) and DR17 (purple squares), vs. log(Ages[yr]), where these ages are provided by Cantat-Gaudin et al. (2020). The green dotted–dashed line and purple dashed line represent the linear fit for DR14 and DR17, respectively. The plot shows a systematic shift from DR14 data to DR17 data.

3.2. The DR17 [C/N] Abundance/Age Calibration

In log–log space the relationship between stellar age and [C/N] appears to be linear; our best fit is given by

$$\log[\mathrm{Age(yr)}]_{\mathrm{DR17}} = 10.14\,(\pm 0.08) + 2.23(\pm 0.19)\,[\mathrm{C/N}] \tag{1}$$

and yields a Pearson coefficient of $R = 0.79$. Our Pearson coefficient is comparable to that found by Casali et al. (2019; $R = 0.85$), although we compute a slightly different offset and a weaker slope.

The linear fit given by Equation (1) and shown in Figure 3 uses Monte Carlo (MC) resampling as described in the fits from Donor et al. (2020). We computed 500 iterations of a linear fit, including uncertainties in the [C/N] abundance ratios and age, and took the mean slope and y-intercept for our final fit, where the respective errors are the standard deviation of the fit.

The discrepancy between our calibration and that of Casali et al. (2019) is partially due to the different APOGEE data sets being used. Casali et al. (2019) used not only DR14 data, but also Gaia-ESO data, and this comparison is shown in Figure 1. Therefore, Figure 4 again reveals the shift in abundance measurements between DR17 and DR14 that was used for the Casali et al. (2019) clusters.

3.3. Common Calibration for RC and RGB Stars?

Stars eventually transition from H-burning on the RGB to He-burning on the RC. Particularly when the He flash is explosive, stars may experience significant mixing that could alter their surface abundances (e.g., Schwab 2020), and therefore the relationship between [C/N] and age. Using the APOGEE-RC catalog (Bovy et al. 2014; J. Bovy et al. 2022, in preparation), we have isolated RC stars from our full sample; once the RC stars are removed, our sample consists of 48 clusters (400 stars) covering an age range of $8.62 \leqslant \log(\mathrm{Age[yr]}) \leqslant 9.89$ and a metallicity range of $-0.53 \leqslant [\mathrm{Fe/H}] \leqslant 0.31$. A new linear fit to this sample yields

$$\log[\mathrm{Age(yr)}]_{\mathrm{DR17,RGB}} = 10.14(\pm 0.07) \\ + 2.22(\pm 0.19)[\mathrm{C/N}] \tag{2}$$

with a Pearson coefficient of 0.81, as shown in Figure 5 (left). This particular calibration yields only a slight change in slope

from the previously found trend (Equation (1)), from 2.23 (± 0.19) to 2.22(± 0.19), but more importantly, the correlation becomes more significant as the Pearson coefficient goes from 0.79 to 0.81.

We then created a sample composed solely of RC stars to investigate whether RC stars follow a similar linear trend of [C/N] abundances and age to that followed by RGB stars. These stars yield a log(Age)–[C/N] relationship that also follows a linear trend with a Pearson coefficient of 0.79:

$$\log[\mathrm{Age(yr)}]_{\mathrm{DR17,RC}} = 10.19(\pm 0.09) \\ + 2.29\,(\pm 0.24)\,[\mathrm{C/N}]. \tag{3}$$

Figure 5 (right) shows the relationship between the [C/N] and log(Age[Gyr]) in our RC cluster sample. The latter comprises 21 clusters (78 stars) covering an age range of $8.62 \leqslant \log(\mathrm{Age[yr]}) \leqslant 9.86$ and a metallicity range of $-0.45 \leqslant [\mathrm{Fe/H}] \leqslant 0.35$. We find that, within the current uncertainties, the relationship for only RGB and only RC stars are the same. We therefore find no evidence for additional significant mixing during the He flash that is affecting the surface C and N abundances for RC stars.

4. Comparison to Previous Work

The recent [C/N]–age calibration by Casali et al. (2019) made use of APOGEE data processed with DR14 analysis software. Moreover, for their calibration Casali et al. (2019) used both Gaia-ESO and APOGEE spectroscopic data along with a literature compilation for cluster ages. In contrast, our analysis here makes use of a uniform sample composed of only APOGEE spectroscopic data, all reduced with the most up-to-date, DR17 reduction of those data, and the most recent Cantat-Gaudin et al. (2020) uniformly determined cluster ages. Thus, it would not be surprising to find significant differences between the Casali et al. (2019) relationship and that derived here. However, surprisingly, their relationship, log[Age(yr)]= 10.54(± 0.06) + 2.61(± 0.10)[C/N], is in fair agreement with our own.

As another means to verify the reliability of our methodology, we can compare predicted stellar ages from our [C/N] calibration to ages independently derived using asteroseismology. For this purpose, we exploit the APOKASC catalog (Pinsonneault et al. 2018). However, because the chemistry used by APOKASC is based on APOGEE DR16 data, we generate age calibrations with respect to DR16 data using the same process we used for our DR17 calibrations. The calibrations for the full, RGB, and RC samples are found to be

$$\log[\mathrm{Age(yr)}]_{\mathrm{DR16,all}} = 9.92\,(\pm 0.05) + 1.94\,(\pm 0.15)[\mathrm{C/N}] \tag{4}$$

$$\log[\mathrm{Age(yr)}]_{\mathrm{DR16,RGB}} = 9.89\,(\pm 0.06) + 1.81\,(\pm 0.16)[\mathrm{C/N}] \tag{5}$$

$$\log[\mathrm{Age(yr)}]_{\mathrm{DR16,RC}} = 9.88\,(\pm 0.07) + 1.94\,(\pm 0.25)[\mathrm{C/N}]. \tag{6}$$

We apply these DR16 full, RGB, and RC sample calibrations and the DR17 full, RGB, and RC sample calibrations (Equations (1)–(3), respectively) on field stars within the APOKASC sample and compare the [C/N]-based stellar ages using our calibrations to the astroseismology-based stellar ages determined by APOKASC. We find the [C/N]-based ages are
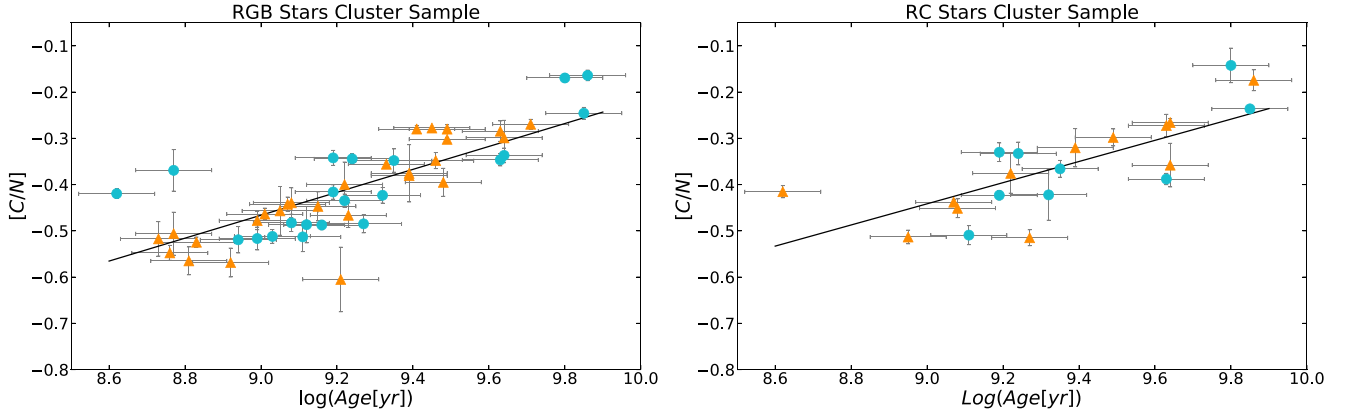
Figure 5. (left) [C/N] abundances vs. log(Age[yr]) for our cluster sample using only RGB stars from 46 clusters common to the OCCAM Survey and the Cantat-Gaudin data set. (right) The [C/N] abundance vs. log(Age[yr]) for clusters containing only RC stars in common between the OCCAM Survey and Cantat-Gaudin data set, which includes 21 clusters. Labels and calculation of calibrations are similar to Figure 3.
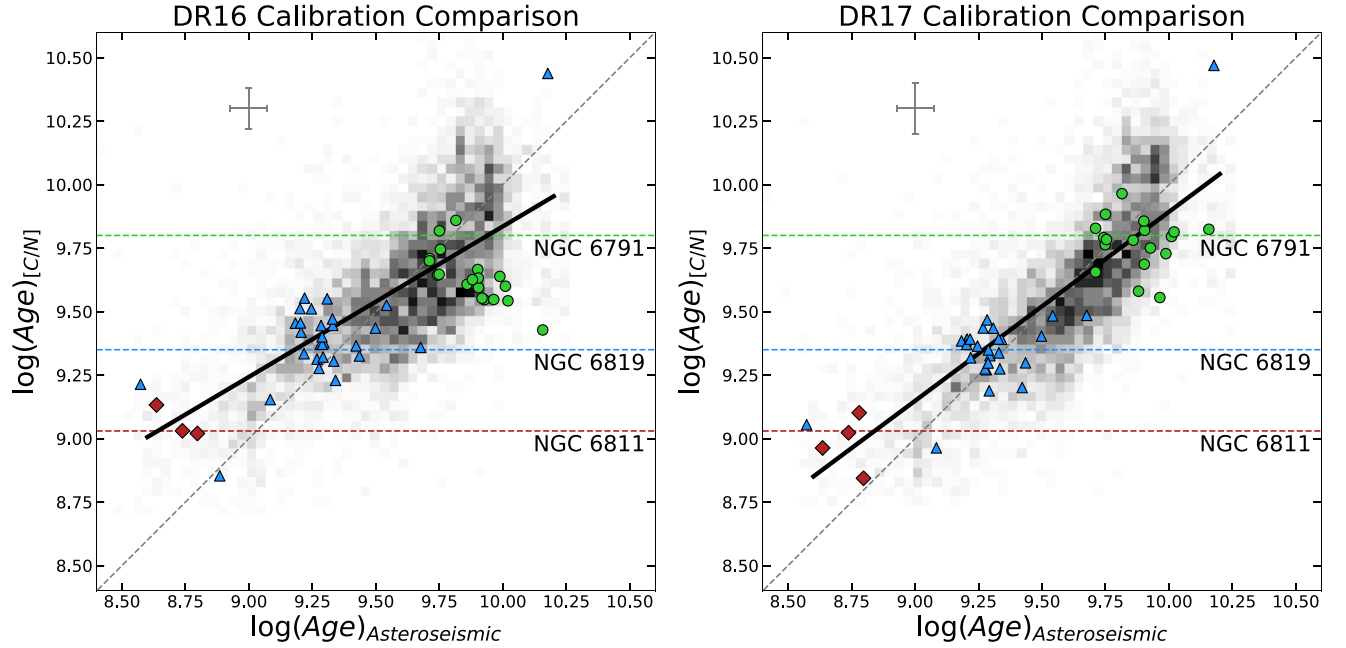
Figure 6. A comparison between our DR16-based age calibration (left) and DR17-based age calibration (right) to asteroseismically determined ages from the APOKASC catalog (Pinsonneault et al. 2018). The gray-gradient shaded regions represent bins of field stars. The green circles, blue triangles, and red diamonds represent cluster member stars common to both samples for NGC 6791, NGC 6819, and NGC 6811, respectively. The horizontal dashed lines are the ages determined by Cantat-Gaudin et al. (2020) for each cluster. The diagonal dashed gray line represents the one-to-one relationship. The solid black line is the linear fit to the main trend of the field stars. Mean representative error bars are shown in each panel.

more consistent with the asteroseismic ages when the newer DR17 calibration is used (see Figure 6), which suggests that the inferred [C/N] values have improved with time and that the newer DR17 data should be preferred.

For further verification, we apply our calibrations to open clusters that are also in the APOKASC sample: NGC 6791, NGC 6819, and NGC 6811. We find that our calculated ages from the DR17 calibration are closer to the ages determined in Cantat-Gaudin et al. (2020) for all three clusters. The spread in the [C/N] calibration ages is due to the uncertainty of [C/N] in the individual cluster members, but such a spread is expected because our calibration is based on the average [C/N] abundance of the cluster. Comparison with these asteroseismic results suggests that [C/N]-based ages can be trusted to 10% for 99.79% of giants, as shown in Figure 6.

On the upper giant branch, above the so-called "red bump," extra convective mixing can occur, particularly in low-metallicity ([Fe/H] $\lesssim -0.5$) stars (Gratton et al. 2000; Shetrone et al. 2019). In principle, this would significantly impact the ages inferred for these stars, making them appear to be younger than they actually are. For this reason, we caution again extrapolating our results too far outside the calibration metallicity range $-0.53 \lesssim$ [Fe/H] $\lesssim 0.31$, particularly for stars on the upper red giant branch.

5. Conclusions

The [C/N] age-dating technique, applicable to RGB stars, has brought a powerful and versatile tool that can be applied to huge numbers of Galactic field stars explored by large-scale spectroscopic surveys with which these two chemical species

can be measured, such as APOGEE DR17. In this work, we have used open cluster ages to calibrate [C/N] as a chemical clock for evolved stars, specifically for the SDSS/APOGEE survey.

1. This calibration, based on APOGEE DR17, provides the following relation for all evolved stars that experience the first dredge-up (e.g., APOGEE DR17 stars with $\log g < 3.3$):

$$\log[Age(\mathrm{yr})] = 2.23\,(\pm 0.19)[\mathrm{C/N}] + 10.14\,(\pm 0.08). \quad (7)$$

This calibration is found to be independent of metallicity of the range explored, $-0.5 \leqslant [\mathrm{Fe/H}] \leqslant +0.3$, with our sample. The calibration is consistent, though slightly different, with the [C/N]–age calibration using DR14 and Gaia-ESO by Casali et al. (2019), which is primarily due to differences in the C and N abundance determination between DR14 and DR17. We also determined the calibration for DR16, which is presented in Section 4.

2. We show that the relationship between age and [C/N] for massive ($M \geqslant 2.5\ M_\odot$) young ($\log(\mathrm{Age}) < 8.5$) giants does not follow the same trend as the relationship calibrated for older, lower-mass giants here. We therefore caution that our relationship should not be extrapolated to this regime.

3. We find that RC stars can be fit with the same calibration as RGB stars. Therefore, we see no evidence for significant extra mixing that affects C and N on the upper RGB or during the He flash for low-mass metal-rich giants. These results align with the findings of Shetrone et al. (2019). With this in mind, we caution the reader not to extrapolate the calibration to lower metallicities ([Fe/H] $\lesssim -0.5$), where potential extra mixing might have a significant impact in measured elemental abundances.

4. Comparison with asteroseismic results suggests that [C/N]-based ages can be trusted to 10% for 99.79% of giants, opening up an exciting future for the estimation of *precise* and *accurate* ages for hundreds of thousands of evolved stars across the Galaxy.

ORCID iDs

Taylor Spoo ● https://orcid.org/0000-0003-4019-5167
Jamie Tayar ● https://orcid.org/0000-0002-4818-7885
Peter M. Frinchaboy ● https://orcid.org/0000-0002-0740-8346
Natalie Myers ● https://orcid.org/0000-0001-9738-4829
Steven R. Majewski ● https://orcid.org/0000-0003-2025-3147
Dmitry Bizyaev ● https://orcid.org/0000-0002-3601-133X
D. A. García-Hernández ● https://orcid.org/0000-0002-1693-2721
Henrik Jönsson ● https://orcid.org/0000-0002-4912-8609

Richard R. Lane ⓘ https://orcid.org/0000-0003-1805-0316
Kaike Pan ⓘ https://orcid.org/0000-0002-2835-2556
Penélope Longa-Peña ⓘ https://orcid.org/0000-0001-9330-5003
A. Roman-Lopes ⓘ https://orcid.org/0000-0002-1379-4204

References

Abdurro'uf, Accetta, K., Aerts, C., et al. 2022, ApJS, 259, 35
Abolfathi, B., Aguado, D. S., Aguilar, G., et al. 2018, ApJS, 235, 42
Ahumada, R., Allende Prieto, C., Almeida, A., et al. 2020, ApJS, 249, 1
Astropy Collaboration, Price-Whelan, A. M., Sipőcz, B. M., et al. 2018, AJ, 156, 123
Astropy Collaboration, Robitaille, T. P., Tollerud, E. J., et al. 2013, A&A, 558, A33
Auvergne, M., Bodin, P., Boisnard, L., et al. 2009, A&A, 506, 411
Baratella, M., D'Orazi, V., Carraro, G., et al. 2020, A&A, 634, A34
Beaton, R. L., Oelkers, R. J., Hayes, C. R., et al. 2021, AJ, 162, 6
Bertelli Motta, C., Salaris, M., Pasquali, A., & Grebel, E. K. 2017, MNRAS, 466, 2161
Blanton, M. R., Bershady, M. A., Abolfathi, B., et al. 2017, AJ, 154, 28
Borucki, W. J., Koch, D., Basri, G., et al. 2010, Sci, 327, 977
Bovy, J., Nidever, D. L., Rix, H.-W., et al. 2014, ApJ, 790, 127
Bowen, I. S., & Vaughan, A. H. J. 1973, ApOpt, 12, 1430
Cantat-Gaudin, T., Anders, F., Castro-Ginard, A., et al. 2020, A&A, 640, A1
Casali, G., Magrini, L., Tognelli, E., et al. 2019, A&A, 629, A62
Cunha, K., Smith, V. V., Johnson, J. A., et al. 2015, ApJL, 798, L41
Danchi, W. C., Lopez, B., Schneider, J., et al. 2006, in IAU Coll. 200, Direct Imaging of Exoplanets: Science & Techniques, ed. C. Aime & F. Vakili (Cambridge: Cambridge Univ. Press), 65
Dearborn, D. S. P., & Eggleton, P. P. 1976, QJRAS, 17, 448
Dearborn, D. S. P., Eggleton, P. P., & Schramm, D. N. 1976, ApJ, 203, 455
Donor, J., Frinchaboy, P. M., Cunha, K., et al. 2018, AJ, 156, 142
Donor, J., Frinchaboy, P. M., Cunha, K., et al. 2020, AJ, 159, 199
Eisenstein, D. J., Weinberg, D. H., Agol, E., et al. 2011, AJ, 142, 72
Frinchaboy, P. M., Thompson, B., Jackson, K. M., et al. 2013, ApJL, 777, L1
Gao, X., Lind, K., Amarsi, A. M., et al. 2018, MNRAS, 481, 2666
García Pérez, A. E., Allende Prieto, C., Holtzman, J. A., et al. 2016, AJ, 151, 144
Gaulme, P., McKeever, J., Jackiewicz, J., et al. 2016, ApJ, 832, 121
Gilmore, G., Randich, S., Asplund, M., et al. 2012, Msngr, 147, 25
Gratton, R. G., Sneden, C., Carretta, E., & Bragaglia, A. 2000, A&A, 354, 169
Gunn, J. E., Siegmund, W. A., Mannery, E. J., et al. 2006, AJ, 131, 2332
Gustafsson, B., Edvardsson, B., Eriksson, K., et al. 2008, A&A, 486, 951
Hasselquist, S., Holtzman, J. A., Shetrone, M., et al. 2019, ApJ, 871, 181
Holtzman, J. A., Hasselquist, S., Shetrone, M., et al. 2018, AJ, 156, 125
Holtzman, J. A., Shetrone, M., Johnson, J. A., et al. 2015, AJ, 150, 148
Hubeny, I., Allende Prieto, C., Osorio, Y., & Lanz, T. 2021, arXiv:2104.02829
Huber, D., Zinn, J., Bojsen-Hansen, M., et al. 2017, ApJ, 844, 102
Iben, I. J. 1964, ApJ, 140, 1631
Iben, I. J. 1965, ApJ, 142, 1447
Iben, I. J. 1967a, ApJ, 147, 624
Iben, I. J. 1967b, ApJ, 147, 650
Jönsson, H., Allende Prieto, C., Holtzman, J. A., et al. 2018, AJ, 156, 126
Jönsson, H., Holtzman, J. A., Allende Prieto, C., et al. 2020, AJ, 160, 120
Kounkel, M., Covey, K. R., Stassun, K. G., et al. 2021, AJ, 162, 184
Magrini, L., Smiljanic, R., Lagarde, N., et al. 2021, Msngr, 185, 18
Majewski, S. R., Schiavon, R. P., Frinchaboy, P. M., et al. 2017, AJ, 154, 94
Martell, S. L., Sharma, S., Buder, S., et al. 2017, MNRAS, 465, 3203
Martig, M., Fouesneau, M., Rix, H.-W., et al. 2016, MNRAS, 456, 3655
Masseron, T., & Gilmore, G. 2015, MNRAS, 453, 1855
Mészáros, S., Allende Prieto, C., Edvardsson, B., et al. 2012, AJ, 144, 120
Myers, N. R., Frinchaboy, P. M., Donor, J., et al. 2022, AJ, submitted
Ness, M., Hogg, D. W., Rix, H. W., et al. 2016, ApJ, 823, 114
Nidever, D. L., Holtzman, J. A., Allende Prieto, C., et al. 2015, AJ, 150, 173
Osorio, Y., Allende Prieto, C., Hubeny, I., Mészáros, S., & Shetrone, M. 2020, A&A, 637, A80
Pinsonneault, M. H., Elsworth, Y. P., Tayar, J., et al. 2018, ApJS, 239, 32
Plez, B. 2012, Turbospectrum: Code for Spectral Synthesis, Astrophysics Source Code Library, ascl:1205.004
Ricker, G. R., Winn, J. N., Vanderspek, R., et al. 2015, JATIS, 1, 014003
Santana, F. A., Beaton, R. L., Covey, K. R., et al. 2021, AJ, 162, 6
Schwab, J. 2020, ApJL, 901, L18
Shetrone, M., Bizyaev, D., Lawler, J. E., et al. 2015, ApJS, 221, 24
Shetrone, M., Tayar, J., Johnson, J. A., et al. 2019, ApJ, 872, 137
Smith, V. V., Bizyaev, D., Cunha, K., et al. 2021, AJ, 161, 254
Spina, L., Nordlander, T., Casey, A. R., et al. 2020, ApJ, 895, 52
Wilson, J. C., Hearty, F. R., Skrutskie, M. F., et al. 2019, PASP, 131, 055001
Zamora, O., García-Hernández, D. A., Allende Prieto, C., et al. 2015, AJ, 149, 181
Zasowski, G., Cohen, R. E., Chojnowski, S. D., et al. 2017, AJ, 154, 198
Zasowski, G., Johnson, J. A., Frinchaboy, P. M., et al. 2013, AJ, 146, 81
Zinn, J. C., Pinsonneault, M. H., Huber, D., et al. 2019, ApJ, 885, 166